2.1 Optical and mechanical design of the extreme AO coronagraphic instrument MagAO-X Preship Review

Laird M. Close[1a], Jared R. Males[a], Alex Hedglen[b], Kyle Van Gorkom[b],
Olivier Durney[a], Corwynn Sauve[a],
Maggie Kautz[b], Lauren Schatz[b], Jennifer Lumbres[b],
Kelsey Miller[b], Victor Gasho[a]

[a] Steward Observatory, University of Arizona, Tucson AZ 85721, USA;
[b] College of Optical Sciences, University of Arizona, 1630 E University Blvd, Tucson, AZ 85719.

ABSTRACT

Here we review the current optical mechanical design of MagAO-X. The project is at the preship review level and has finished the design phase. The design presented here is the baseline to which all the optics and mechanics have been fabricated. The optical/mechanical performance of this novel extreme AO design will be presented here for the first time. Some highlights of the design are: 1) a floating, but height stabilized, optical table; 2) a woofer/ tweeter design (2040 actuator BMC MEMS tweeter DM with an ALPAO DM97 woofer DM); 3) 22 very compact optical mounts that have a novel locking clamp for additional thermal and vibrational stability; 4) A series of four pairs of super-polished off-axis parabolic (OAP) mirrors with a relatively wide FOV by matched OAP clocking; 5) an advanced very broadband (0.5-1.7μm) ADC design; 6) A Pyramid (PWFS), and post-coronagraphic LOWFS NCP wavefront sensor; 7) a vAPP coronagraph for starlight suppression very close-in to the star; 8) Twin science cameras to have twice the telescope efficiency and allow higher contrasts with simultaneous differential imaging (SDI). Currently MagAO-X is completely fabricated and tested in the lab. It is ready for preship review and then (pending a positive outcome shipping to Chile) for first light in December 2019 at the 6.5m Clay telescope.

Keywords: Extreme AO; High-contrast imaging; Optics; Mechanics; Woofer-Tweeter;

1.0 INTRODUCTION

1.1 Introduction to MagAO-X

MagAO-X is a unique ExAO system in that it has been targeted for primarily doing coronagraphic science in the visible part (0.5-1.0 μm) of the spectrum. This is in contrast to many of today's ExAO systems that target the NIR (1-2.4 μm) for coronagraphy like GPI and SPHERE. MagAO leverages the excellent Las Campanas site and the slightly smaller D=6.5m size of the Magellan (Clay) telescope to allow excellent Strehls in the optical.

By use of 1700 corrected modes (at 3.7 kHz) from an advanced woofer-tweeter design we predict Strehls of ~70% at Hα (0.6563 μm) in median seeing conditions --see Males et al. 2018 for detailed simulations of the performance of MagAO-X.

1.2 Scientific Advantages to Visible AO

Despite its demanding nature, visible AO has many scientific advantages over the NIR. After all, most astronomy is done in the visible, but almost no AO science was done with λ<1μm on large 6.5-10m class telescopes until recently (Close et al. 2018; these proc.). A short list of some of the advantages of AO science in the visible compared to the NIR are:

-- **Better science detectors** (CCDs): much lower dark current, lower readnoise (<1e- with EMCCDs), much better cosmetics (no bad pixels), ~40x more linear, and camera optics can be warm, simple, and compact.

[1] lclose@as.arizona.edu; phone +1 520 626 5992

-- **Much Darker skies:** the visible sky is 100-10,000x darker than the K-band sky.
-- **Strong Emission lines**: access to the primary visible recombination lines of Hydrogen (Hα 0.6563 μm) --- most of the strongest emission lines are all in the visible, and these have the best calibrated sets of astronomical diagnostics. For example, the brightest line in the NIR is Paβ some *20 times less strong* than Hα (in typical Case-B recombination conditions, T~10,000K).
-- **Off the Rayleigh-Jeans tail**: Stars have much greater range of colors in the visible (wider range color magnitudes) compared the NIR which is on the Rayleigh-Jeans tail. Moreover, visible photometry combined with the IR enables extinction and spectral types to be much better estimated.
-- **Higher spatial resolution**: The 20 mas resolution regime opens up. A visible AO system at r band (λ=0.62μm) on a 6.5m telescope has the spatial resolution of ~20 mas (with full *uv* plane coverage unlike an interferometer) that would otherwise require a 24m ELT (like the Giant Magellan Telescope) in the K-band. So visible AO can produce ELT like NIR resolutions on today's 6.5-8m class telescopes.

1.3 Keys to good AO Performance in the Visible: Some "point design" considerations for MagAO-X

While it is certainly clear that there are great advantages to doing AO science in the visible it is also true that there are real challenges to getting visible AO to produce even moderate Strehls on large telescopes. The biggest issue is that r_o is small ~15-20 cm in the visible (since $r_o=15(\lambda/0.55)^{6/5}$ cm on 0.75" seeing site). Below we outline (in rough order of importance) the most basic requirements to have a scientifically productive visible AO system on a 6.5m sized telescope:

1. **Good 0.6" V-band Seeing Site** – Large r_o (>15cm at 0.55μm) and consistency (like clear weather) is critical. In particular, low wind (long τ_o > 5ms) sites are hard to find, and so this drives loop WFS update frequencies ≥1 KHz (due in large part to the fast jet stream level winds).

→ *We have a 3.7 kHz 120x120 OCAM2 PWFS to overcome this, and our site is excellent with median 0.6" seeing.*

2. **Good DM and fast non-aliasing WFS**: need many (>500) actuators (with $d<r_{o/2}$ sampling), no illuminated "bad/stuck" actuators, need at least ≥300 well corrected modes for D>6m. Currently the pyramid WFS (PWFS) is the best for NGS science (uses the full pupil's diffraction for wavefront error measurement), hence a PWFS is preferred.

→ *We have a 2040 actuator BMC 2Kilo DM tweeter (3.5μm stroke) with only one bad "bump" over 2 actuators being controlled with up to 1700 modes by a PWFS.*

3. **Minimize all non-common path (NCP) Errors:** Stiff "piggyback" design with visible science camera well coupled to the WFS –keep complex optics (like the ADC) on the common path. Keep optical design simple and as common as possible. Limit NCP errors to less than 30 nm rms. If the NCP errors are >30 nm rms employ an extra non-common path DM to fix these errors feed by a LOWFS sensor (see Males et al. 2018; these proc).

→ *We have minimized the number of non-common optics to just 3 super-polished (λ/40 P-V; 0.1 nm roughness) flat mirrors, and one similar quality OAP. Hence, we expect less than ~30 nm of NCP, but have plans for an extra NCP correcting (NCPC) DM. That extra NCPC DM (another ALPAO DM-97) would be fed by a low-order WFS (LOWFS) that is directly at the coronagraphic focal plane (Miller et al. 2018 these proc).*

4. **Minimize the Low Wind Effect (LWE):** This is a wavefront error that is linked to the strong radiative cooling of the secondary support spiders in low wind. It can be mostly removed by adding a low emissivity coating so that the spiders track the temperature of the night air. Also a pyramid wavefront (PWFS) sensor seems much better at sensing the LWE errors compared to SH WFS according to Milli et al. 2018 (these proc).

→ *We never see LWE with MagAO currently, but if it becomes as issue with MagAO-X we expect the PWFS to sense it and the tweeter to eliminate it. We not expecting LWE to be a problem for MagAO-X*

5. **Minimize the Isolated Island Effect**: Unfortunately, the push towards having many corrected modes (~1700 for MagAO-X) forces visible AO systems to small subap sizes (13.5cm for MagAO-X) that approach spiders arm thicknesses (1.9 and 3.81 cm at Magellan). Hence some sub-apertures are mostly in the shadow of the spider arms and so cannot be effectively used by the WFS, allowing the DM to "run-away" in piston w.r.t. each "isolated" quadrant/section of the pupil (see Obereder et al. 2018 these proc.). This is an insidious problem which favors the use of PWFSs (which could, in theory, sense the phase difference between the quadrants in these dark zones). However, it is still unclear if PWFS can actually measure these phase differences if they are also dominated by other wavefront errors. Moreover, if the phase differences are greater than 2π the PWFS needs additional support or it will converge to the wrong (modulo 2π) solution (Esposito et al. 2017) and so an additional PWFS at another

wavelength, or a real-time interferometer like a Zernike sensor (ZELDA; N'Diaye et al. 2017), or phase diversity in science focal plane; N'Diaye et al. 2018; (these proc.) must be used. This is not a solved problem on-sky.
→ *Extensive lab tests with realistic spider thicknesses show no sign of this effect, so MagAO-X may not have to deal with this issue.*
4. **Lab Testing:** Lots (and lots) of "end-to-end" closed loop testing with visible science camera. Alignment must be excellent and very stiff for all non-common path optics (for all observing conditions) to minimize NCP errors.
→ *In PI Jared Males' lab we have fully simulated telescope feeding MagAO-X in a clean room. Closed-loop tests will continue until into early 2019. We will ship MagAO-X back to the lab for further tests after each run in Chile.*
5. **Modeling/Design:** Well understood error budget feeding into analytical models, must at least expect ~60 nm rms WFE on-sky. Try to measure/eliminate vibrations from the telescope and environment with advanced rejection/filter techniques (eg. linear quadratic estimation (LQG) filters).
→ *PI Males has a full closed loop model of MagAO-X performance. And we have full Fresnel propagation of each optical surface to assess the coronagraphic performance of the system (see Lumbres et al. 2018 these proc).*
6 **High Quality Interaction Matrixes:** Excellent on-telescope IMATs with final/on-sky pupil. Take IMATs in partial low-order closed-loop to increase the SNR of the high order modes in the IMAT.
→ *We will be able to obtain high SNR IMATs internally with MagAO-X and test them rigorously with our turbulence simulator in the lab or even at the telescope.*
7 **IR camera simultaneous with Visible AO camera:** this is important since you achieve a 200% efficiency boost. Allows for excellent contingency in poor seeing when only NIR science is possible.
→ *the NIR is fully corrected by MagAO-X and will feed a future J (and maybe H band) science camera.*
8. **Leverage Differential Techniques for Enhanced Contrasts:** Differential techniques such as Spectra Differential Imaging (SDI) or Polarmetric Differential Imaging (PDI) are very effective in the visible, and when combined with Angular Differential Imaging (ADI) observations with Principal Component Analysis (PCA) data reduction techniques, can lead to very high contrast detections of 10^{-5} within 100mas (Males et al. 2016).
→ *MagAO-X has an excellent ADC, K-mirror, and pupil tracking loop which all together will enable long (~8 hour) pupil stabilized coronagraphic visits to targets. We will also increase contrast initially by carving a dark hole with a vAPP coronagraph (Otten et al. 2017). We expect 10^{-4} (raw 1s exposure) contrasts at 100mas at Hα for faint R=10 mag guides stars (Males et al. 2016). Then the final boost in contrast will come from our dual camera SDI design where, say, Hα and nearby continuum images can be imaged simultaneously. Then post-processing with KLIP/PCA can be used to calibrate and remove the PSF from each SDI science arm. The final SDI subtraction of Hα – continuum should detect Hα planets at 5σ at contrasts of 10^{-5} - 10^{-6} at 100mas in ~1 hour.*

2.0 OPTICAL MECHANICAL DESIGN

For coronagraphy MagAO-X needs to minimize the vibrations on the optical table. We have selected a design solution where the instrument is self-contained in an enclosed floating (gravity invariant) optical table. The air dampening of the table will eliminate high frequency (>5Hz) vibrations from the telescope environment coupling into the instrument. However, a floating table might have low amplitude rocking at ~1Hz due to wind load etc. Hence, the rest of the MagAO-X's opto-mechanical systems (table, optical mounts, wheels etc.) are designed to be stiff enough to allow a <5 Hz solid body motion of the entire table without exciting jitter. This is critical for good coronagraphic performance. We have selected to have the actual height of the optical table to controlled, close-loop, by capacitive sensors mounted under the table. To our knowledge this is the first time this particular technical solution has been attempted at a telescope (although SPHERE has a somewhat similar system; Beuzit, J-L. private comm.).

Optically we have tried to minimize the size of the instrument, this led to a 2 tiered optical layout with some folds for compactness. We needed an excellent all reflective design so that science could be done from 0.5-1.8μm. We needed 4 pairs of super-polished OAP relays to produce 4 pupils (#1 Alpao woofer pupil (13.1mm); #2 BMC DM Tweeter pupil (18.8mm); #3 PWFS modulator/coronagraphic pupil (9.0mm); and #4 the Lyot stop pupil (9.0 mm)). We also have 5 focal planes (#1 f/11 telescope FP; #2 f/16 FP; #3 f/57 FP; #4 f/69 PWFS/Coronagraphic mask FP; #5 final f/69 post-coronagraphic science FP (6x6" FOV)). The optical design is nearly perfect even over very broadband at high

airmasses thanks to our ADC design. The conceptual design of MagAO-X is shown below in a simple cartoon:

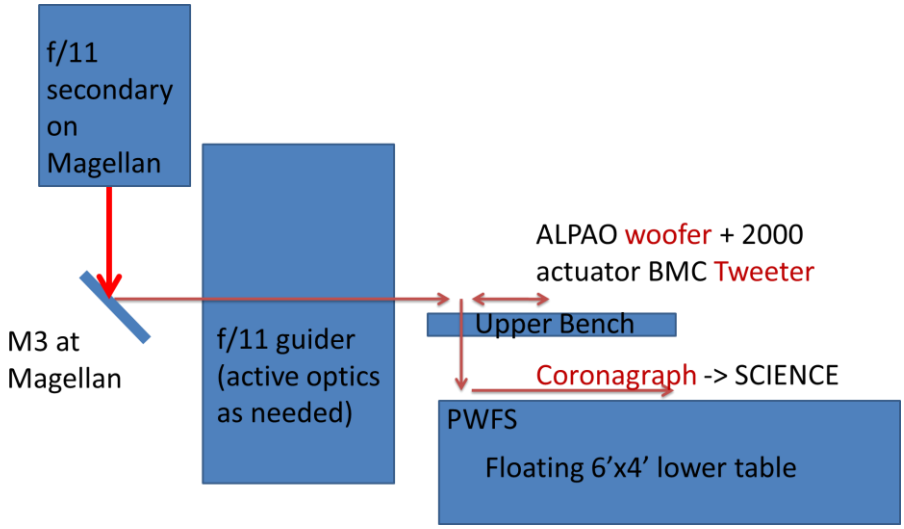

The details of the actual design can be found below in Figs. 1, 2 and 3. The optical performance is shown in Fig. 4a and 4b. Note the excellent predicted performance over 0.5-1.7μm even at high airmass.

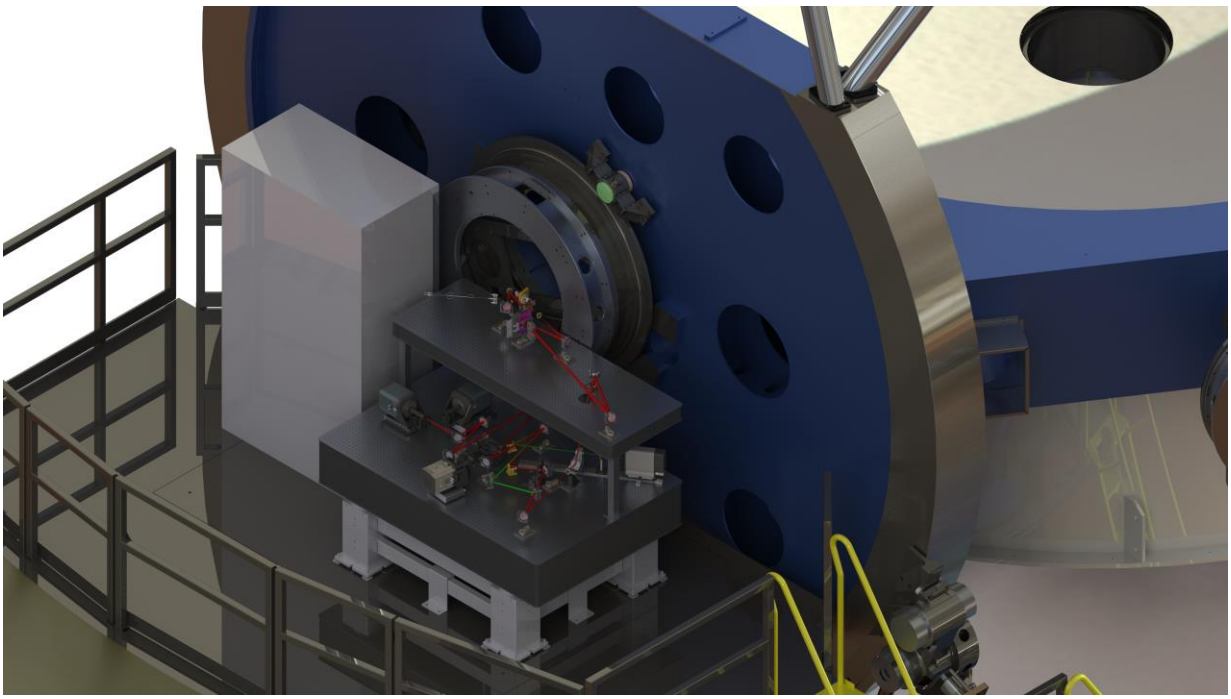

Fig. 1: MagAO-X as mounted at the 6.5m Magellan telescope's Nasmyth f/11 focus. The large, glycol cooled, rack to the left is for the all the MagAO-X electronics. MagAO-X is gravity invariant and mounted on a floating optical table (so neither flexure nor NCP vibrations >5 Hz are issues). Note, for clarity the dust cover is removed from the instrument. For more details see Males et al. 2018 these proc.

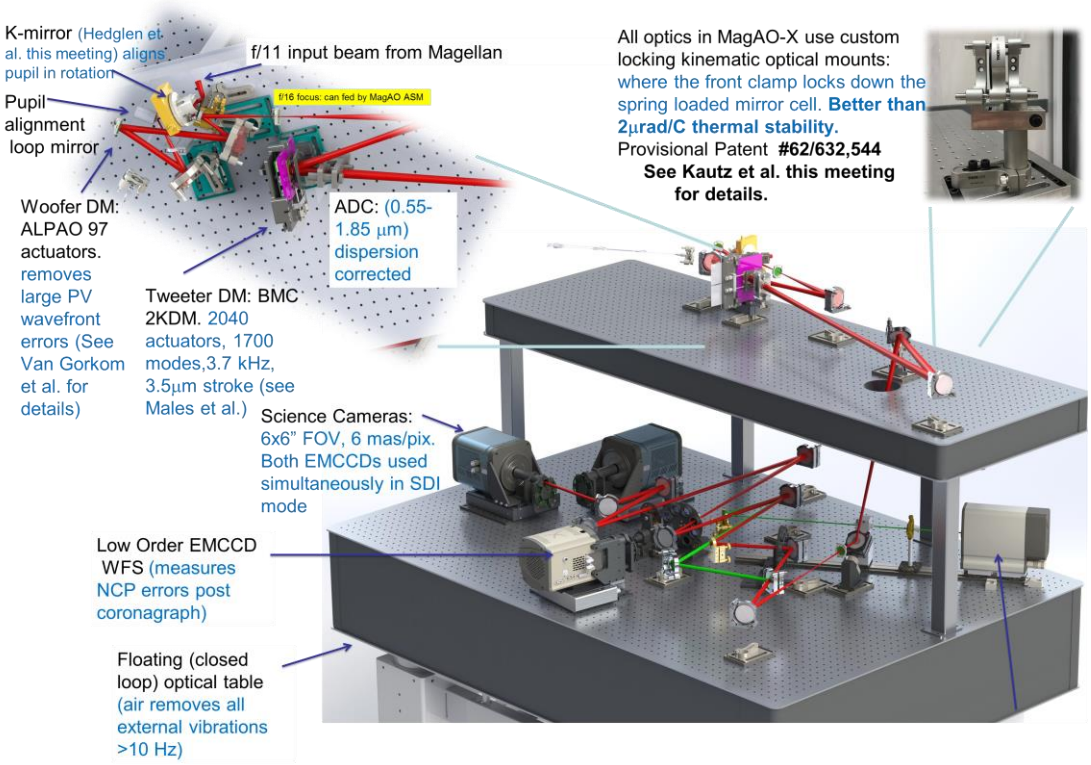

Fig. 2: The optical and Mechanical design for MagAO-X.

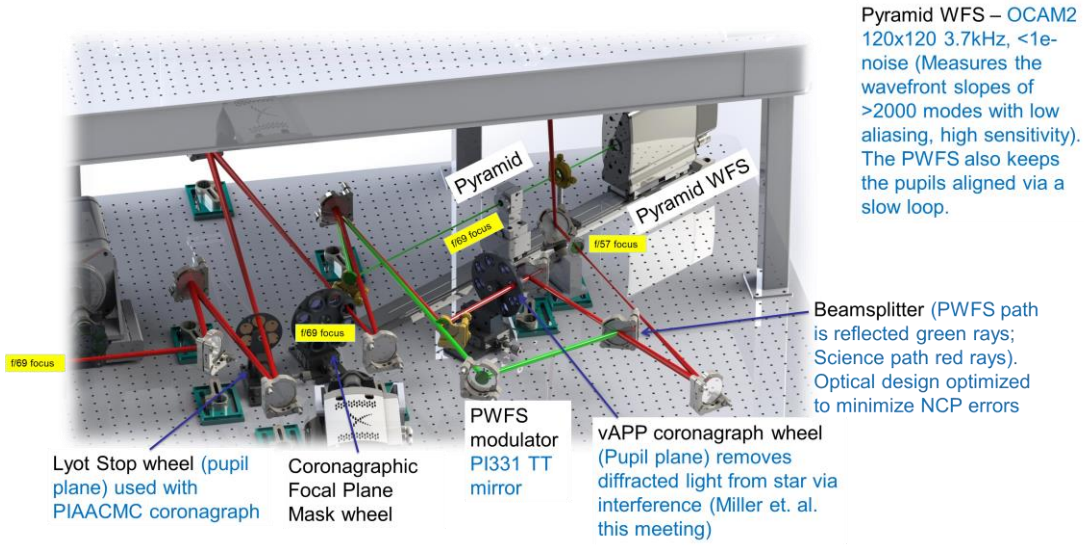

Fig 3: Detail of the MagAO-X vAPP Coronagraphic science (red) and PWFS (green) beam paths.

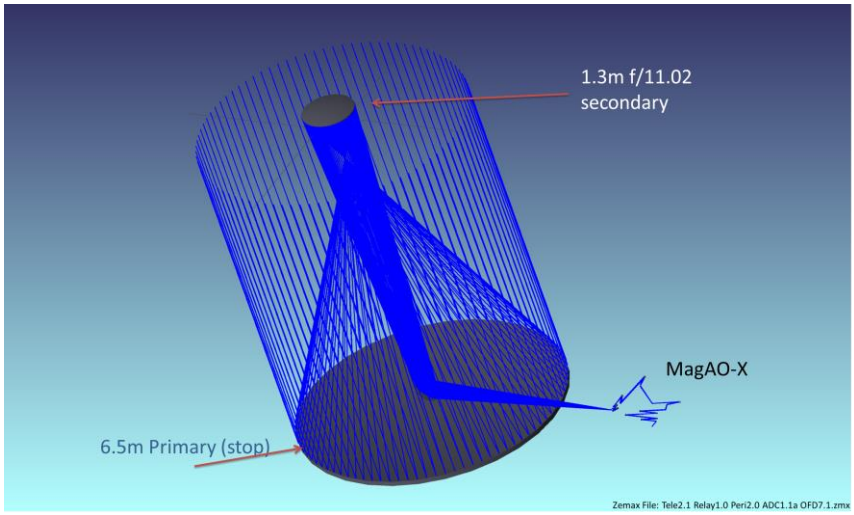

Fig 4a: Detail of the MagAO-X optical design.

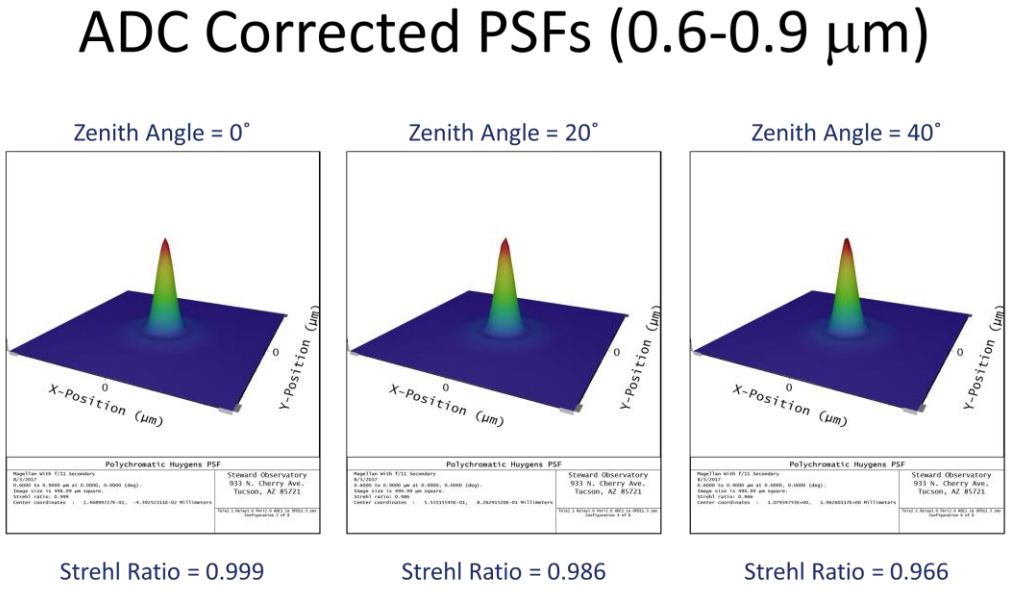

Fig. 4b: Full "end-to-end" optical performance of the MagAO-X optical design. In particular this design corrects atmospheric dispersion from 0.5-1.7μm with an excellent ADC. This design allows a PWFS to work broadband over the entire visible and NIR range (0.5-1.7μm) for a large range of zenith angles. Initially the MagAO-X PWFS with its OCAM2 will just work broadband over 0.55-0.95μm (shown in the polychromatic PSFs above). Of course, over any one single science filter (like r') the Strehl is >99.5% by Zemax.

3.0 STATUS

Currently at the Extreme Wavefront Control Lab (PI Jared Males) at Steward Observatory we have fully assembled the custom floating optical table and have integrated nearly all the optics mechanics and fully tested the entire system (see Fig. 5). All the optics have been delivered in spec. We are currently in the final tuning and detailed testing phase.

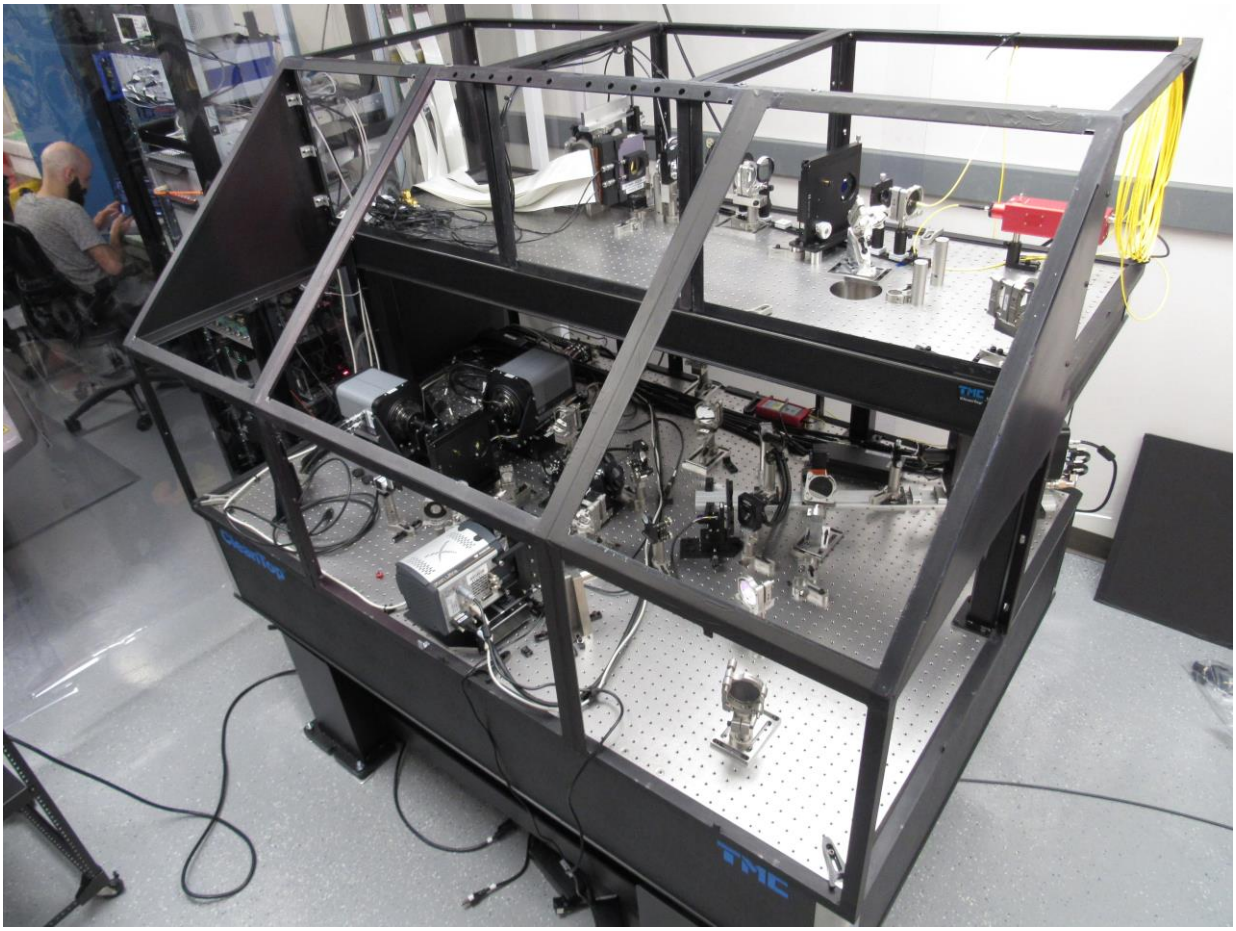

Fig 5: The Current (Aug. 2019) view of the MagAO-X optical table in the Clean Room Steward Observatory's High-Contrast Wavefront Sensing Lab. Kyle Van Gorkom is at the workstation that controls all of MagAO-X. Dust covers off.

Currently we have aligned all the OAPs and other optics to produce the f/69 focal plane on the tip of the pyramid (also this is the same PSF at the coronagraphic mask focal plane). See Figure 6 for an image of this PSF on our science camera. Once the DMs are flatted the PSF Strehl is very high (see right hand of Fig 6). The fabricated stages and custom filter wheels for the 2 science cameras and LOWFS have been integrated on the table. The three custom filter wheels (a vAPP/coronagraph wheel, a focal plane mask wheel, and a Lyot stop wheel) have been assembled, added to the table and tested for optical stability.

We have also added our Alpao DM-97 woofer to the instrument (see Fig 7 and Van Gorkom et al. 2018). Our BMC 2Kilo DM (48.0x47.0 illuminated actuators (AOI of 11.716^{o}) with a ring of 1-1.5 unilluminated edge actuators) has also been fully integrated and tested (see Fig 7 and Males et al. 2018). The tweeter also has a custom designed environmental control system for DM safety which is still in final stages of testing. Currently

MagAO-X is completely operating closed-loop in the lab. We are now doing mock science tests and refining calibrations. The system and all mechanisms works remotely, with no need to open the dust covers, visit instrument for routine science operations.

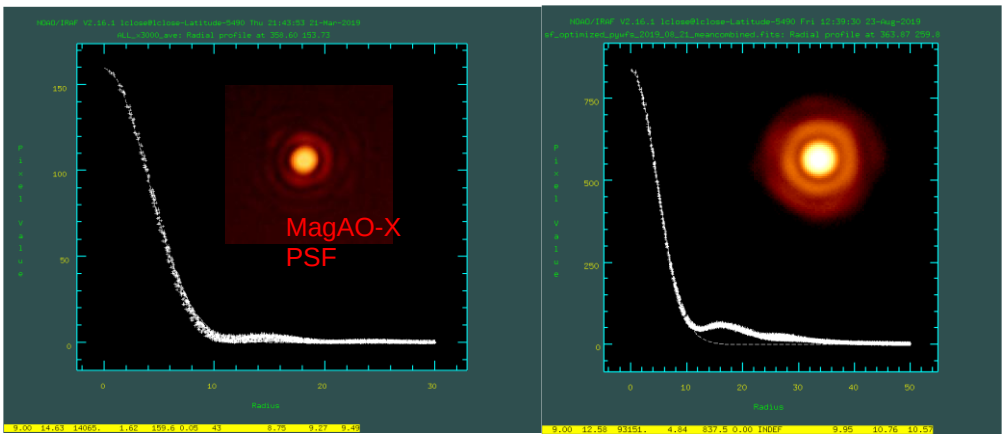

Figure 6 (Top Left): Open-loop non-coronagraphic PSF with 633nm laser. The PSF FWHM at 633nm at the f/69 science focus is 44.50um (exactly that expected for 1.02λ/D unobscured PSF). The peak of the first ring is ~3% max which is close to ~2.5% expected.
Figure 6 (Top right): Open loop PSF with Magellan's pupil and white light (0.6-1.0 microns). The woofer here is set to its "flat position" (see Van Gorkom et al.). This very high SR white light PSF is providing the reference point for AO correction. Note the PSF has a slightly a chromatic focus due to the refractive achromatic (f=250mm doublet) objective of the telescope simulator – this will be naturally removed when observing a star with the real (reflecting) telescope).

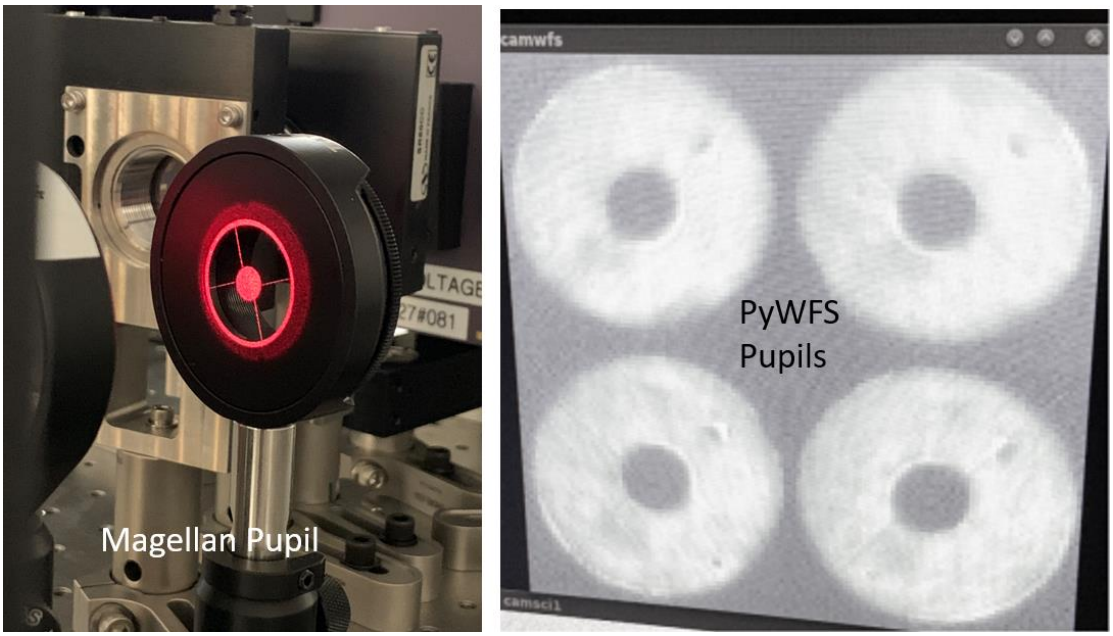

Figure 6 (Bottom left): The Magellan pupil mask. The telescope simulator makes a perfect f/11.02 beam. After the woofer has removed all the low wavefront errors we have very flat wavefronts. Here **(bottom right)** we show the OCAM image of the 4 pupils from the PyWFS (in laser light, with the woofer removing most of the low order errors). Note the flat wavefront and relatively uniform illumination. This provides a good starting calibration point for the taking the AO response matrix in CACAO.

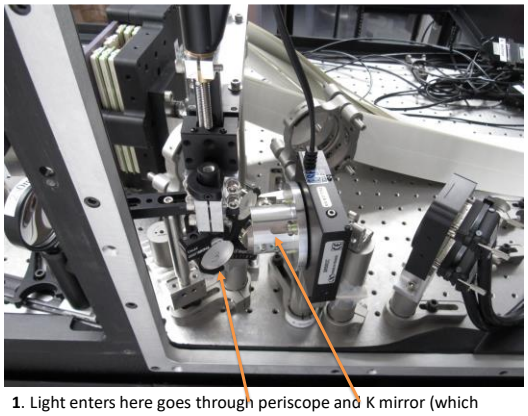

1. Light enters here goes through periscope and K mirror (which stabilizes the telescope pupil for the coronagraph)

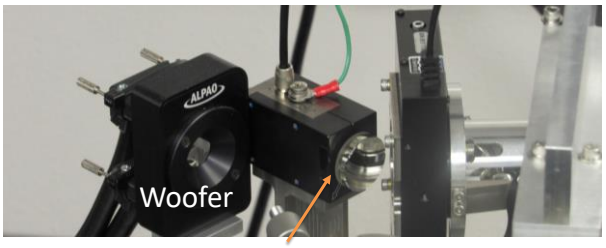

2. Pupil is aligned off pupil TTM (PI 335) then 13.0mm pupil is formed on woofer (11 illuminated actuators, with 0.75mm of unilluminated mirror around edge)

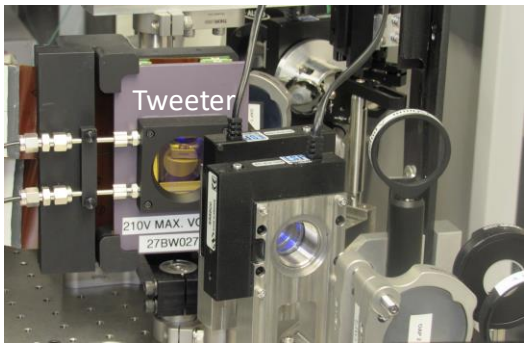

3. 18.8mm Pupil is formed on tweeter (48 x 47 actuators, leaving guard ring of 1.5 unilluminated actuators)

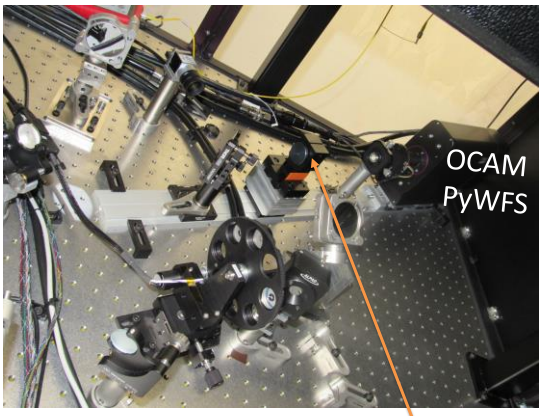

4. The f/69 focal plane is focused on the tip of the pyramid and then 4 pupils are reimaged onto four 56 pixel diameter circles on the 128x128 (bin2) OCAM EMCCD. These pupils allow the wavefront to be measured and a negative feedback loop is close on the woofer/tweeter. The positions of the pupils measured and are held steady by the pupil TTM.

Figure 7: Highlights of the wavefront sensing and correcting path for MagAO-X. Here we see the main components of the main servo loop for MagAO-X. The PyWFS senses the wavefront on the OCAM and commands the tweeter at (3.7kHz framerate) to minimize the deviation from the reference PyWFS "flat" calibration. The tweeter offloads the mean of its shape to the woofer which has ~30um of stroke. Also, the pupil is exactly controlled by the pupil TTM which uses the OCAM pupil measurands to zero out any drift of the pupils at ~1-100 Hz– in this manner the Tweeter pupil is stable to <40 microns.

4.0 CORONAGRAPHIC STARLIGHT SUPPRESSION

Over summer 2018 we finished the final alignment of our PyWFS (see Schatz et al. 2018 for more details). We have aligned our fabricated custom compact K-mirror to the optical table (see Hedglen et al. 2018 for more details) and to the telescope simulator. Today (August 2019) all the optics and the AO and PyWFS servos work as expected for MagAO-X. Here we discuss the last part of the science channel (see Fig 9) that of the coronagraph that is designed to take advantage of the high Strehl of MagAO-X to suppress starlight.

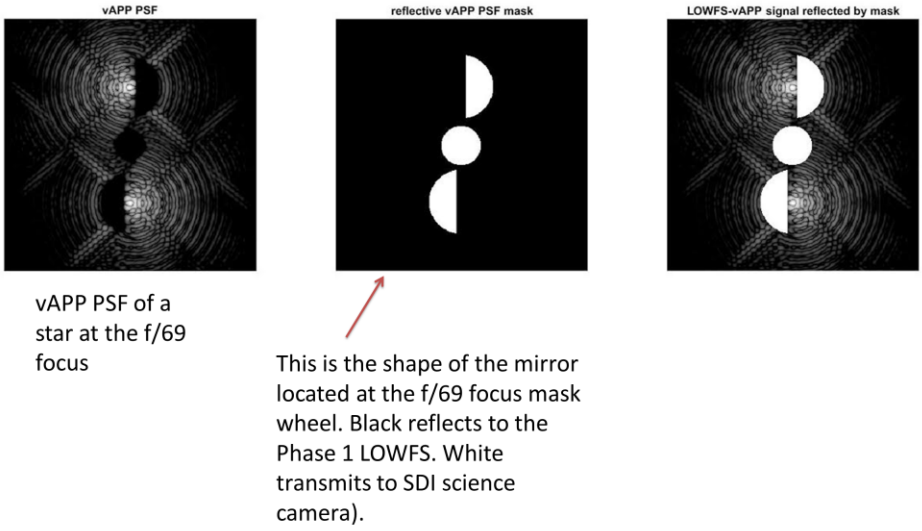

Fig. 8: *(left)* **Narrow band simulations of the vAPP coronagraphic f/69 PSF** (Otten et al. 2017). Note the upper and lower "dark holes". At the coronagraphic focal plane mask wheel (see Fig. 3) we will have a mirror in the shape of the middle panel where black is the reflective surface and white is the transmissive holes (where the high contrast "planet" light passes to the SDI cameras). The right hand image is the input light to the LOWFS for post-coronagraph WFS and NCP sensing. See Miller et al. 2018 for more details. In the dark holes raw (one second exposure) contrasts of 10^{-4} at 100 mas should be obtained as modeled by propagation through the 22 as-built reflective optics in MagAO-X (Lumbres et al. 2018; Males et al. 2018). See figure 9 part 4 for real broadband (i' and z') science vAPP images on the SDI cameras.

The vAPP coronagraphic phase plate is finished and the focal plane masks are in fabrication (Otten et al. 2017; Miller et al. 2018) One of our vAPPs is shown in Fig. 8 in simulation and as optically tested in figure 9.

The NCPC DM needs a WFS to optimize the contrast of the vAPP. The MagAO-X vAPP allows Zernike modal control (ZMWFS), which can allow either the science camera(s) or the LOWFS to sense low order modes in the focal plane of the VAPP (Miller et al. 2018). The coronagraphic vAPP dark hole can also be maintained and enhanced by Linear Dark Field Control (LDFC). For more on our LDFC and ZMWFS lab experiments with an vAPP see Miller et al. 2018. Also to mask the one "bump" on our tweeter DM we have an oversized spider arm in the coronagraphic pupil plane mask (see Fig 9 part 1) this masks the bump but also introduces an asymmetric pupil which allows for phase diversity to work with just the science camera images. So there are many ways to control the NCPC DM with MagAO-X as built, lab testing and on-sky tests will determine the optimal approach.

5.0 SHIPPING & COMMISSIONING

By fall 2019 the MagAO-X system should be ready to ship to Chile (pending a successful preship review) for first light commissioning and science. Our packing and shipping plans are well advanced and have passed a separate external review, and will be looked at again during preship review on Sept. 6, 2019. We refer the reader to the *MagAO-X Shipping Hardware PreShip Review* by Jamison Noenickx and the *MagAO-X Telescope Alignment PreShip Plan* by Laird Close for more details. We note here that the bench optics themselves are well protected for shipping by each expensive item being captured in a locked (paten pending) mount with a Teflon bumper in case of a massive impact during shipping.

6.0 SCIENCE & FUTURE

After the first light run (Dec. 2019) we will add more advanced coronagraphs like a custom PIAACMC coronagraph to increase or contrasts at ~1-2λ/D inner working angles. However, even at first light we fully expect MagAO-X with its vAPP to be an excellent visible wavelength AO coronagraph, and to open new avenues in exoplanets and high-contrast science. For example, in its Hα SDI mode MagAO-X's 10^{-5} contrasts at Hα (0.656μm) at inner working angles of ~60-100 mas will be >100x higher contrast than any other telescope (in space or on the ground) can reach today (or for the foreseeable future). MagAO-X's key project (MaxProtoplanets) survey should allow a ~20x increase in the number of forming protoplanets that can be directly imaged in Hα emission (the current protoplanet sample is just: Lk Ca 15 b Sallum et al. 2015; PDS 70 b Wagner et al. 2018). Hence just this one mode of MagAO-X will illuminate one of the greatest mysteries in astronomy: the exact mechanisms of planet formation. Many other exoplanet and circumstellar disk discoveries awaits MagAO-X.

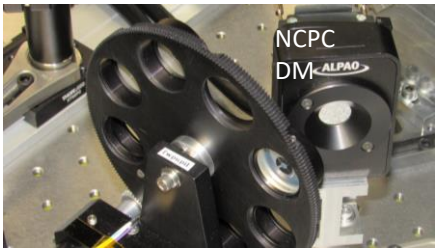

1. AO corrected science path light is removed of all NCP errors by the NCPC DM. It then immediately enters the coronagraph wheel

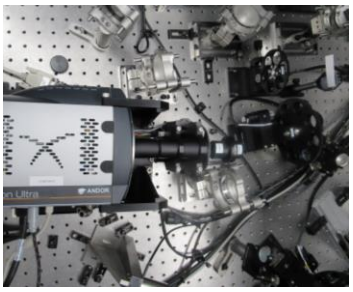

2. The EMCCD LOWFS uses some starlight in a negative feedback loop to sense and remove any NCP errors with the NCPC DM.

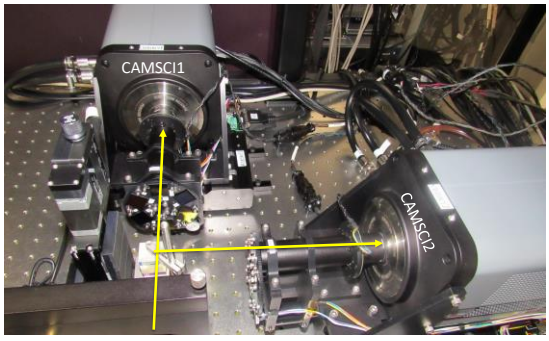

3. The f/69 beam is reimaged onto a pair of EMCCDs with 6x6 FOV and 6mas/pix. The beams are split by an elevator of different custom dichroic cube beam splitters to maximize QE of both cameras.

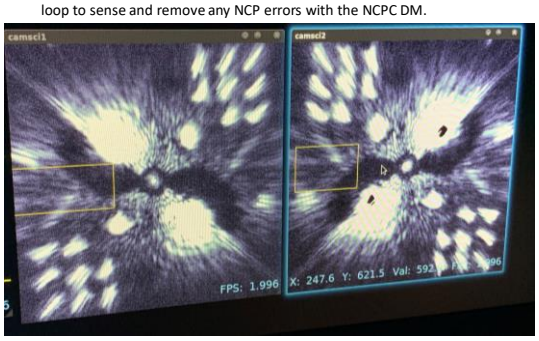

4. vAPP coronagraphic images on the 2 science cameras. On the left we have Camsci1 in the z' filter. On the right we have Camsci2 in the i' filter. Note the very dark (~10^{-4} raw) regions in side the working range of the vAPP even with these very wide filters.

Figure 9: Highlights of the science path for MagAO-X. The science light is transmitted through a dichroic beamsplitter and is corrected for any non-common path (NCP) errors w.r.t. the PyWFS loop. The NCP errors can be calculated from either the Zernike modal spots formed by the vAPP on the science cameras, or by the LOWFS camera at higher rates (~100Hz). The NCPC DM feeds a nearly perfect wavefront to the vAPP coronagraph (in the coronagraph wheel). The light is then reimaged at f/69 to the 2 science cameras. Each science camera makes high contrast images in different wavelengths (like the 10^{-4} raw PSF contrast at ~80 mas shown above in the initial science camera demo).

MagAO-X could not have been possible without support from the NSF's Major Research Infrastructure (MRI) research grant # *1625441 Development of a Visible Wavelength Extreme Adaptive Optics Coronagraphic Imager for the 6.5 meter Magellan Telescope* (PI: Jared Males). L.M.C.'s research was also supported by the NSF AAG program #1615408 (PI Laird Close). Laird Close and Alex Hedglen are supported by the NSF's AAG program #1615408 and NASA's XRP program 80NSSC18K0441 (PI Laird Close).

REFERENCES

Close L.M. et al. 2005b NATURE 433, 286
Close L.M. et al. 2003a, ApJ 599, 537
Close L.M. et al. 2003b ApJ 598, 35L
Close, Laird M.; Gasho, Victor; Kopon, Derek; Males, Jared; Follette, Katherine B.; Brutlag, Kevin; Uomoto, Alan; Hare, Tyson, Adaptive Optics Systems II. Edited by Ellerbroek, Brent L.; Hart, Michael; Hubin, Norbert; Wizinowich, Peter L. 2010 Proceedings of the SPIE, Volume 7736, pp. 773605-12
Close L.M., Males, J. et al. 2013, ApJ, 774 94
Close L.M., Males, J. et al. 2014, ApJ Lett 781 L30
Close L.M., Males, J. et al. (2018) Proc SPIE 10703
Esposito S. et al. 2006 Proc. SPIE Volume 6272, pp. 62720A
Esposito, Simone; et al. Proceedings of the SPIE, Volume 7736, pp. 773609-12
Follette K., Close, L. et al. 2013 ApJ 775, L3
Fortney, J. J.; Marley, M. S.; Saumon, D.; Lodders, K. 2008 The Astrophysical Journal, Volume 683, Issue 2, pp. 1104-1116.
Fraga, Luciano; Kunder, Andrea; Tokovinin, Andrei (2013) AJ 145, 165
Fusco, T. et al. 2016, Proc. SPIE 9909;
Gratadour, D., Rouan, D., Mugnier, L. M., Fusco, T., Clenet, Y., Gendron, E. & Lacombe, F. 2006, A&A, 446, 813G.
Gladysz, S. et al. 2008, PASP, 120, 1132
Guyon, O. Et al. (2018); Proc SPIE 10703
Hedglen, A. et al. (2018) proc SPIE 10703
Kautz M., et al. (2018) proc SPIE 10703
Kopon, Derek; Close, Laird M.; Males, Jared; Gasho, Victor; Follette, Katherine 2010 Adaptive Optics Systems II. Edited by Ellerbroek, Brent L.; Hart, Michael; Hubin, Norbert; Wizinowich, Peter L. Proceedings of the SPIE, Volume 7736, pp. 77362V-11
Kopon, D., Close, L.M., et al 2013 PASP
Lenzen R., et al. 2005 proc "ESO workshop on science with AO", 115
Lloyd-Hart 2000, PASP 112, 264
Lumbres, J. et al. (2018) these Proc.
Macintosh, B.A. et al. 2008 Wizinowich, Peter L. Proceedings of the SPIE, Volume 7015, pp. 701518-13
Males, Jared R.; Close, Laird M.; Kopon, Derek; Gasho, Victor; Follette, Katherine, 2010 Adaptive Optics Systems II. Edited by Ellerbroek, Brent L.; Hart, Michael; Hubin, Norbert; Wizinowich, Peter L. Proceedings of the SPIE, Volume 7736, pp. 773660-13
Males, J.R., Close, L.M. et al 2014 ApJ 786, 42
Males, J.R., Close, L.M., Guyon, O., Morzinski, K., et al. (2016), Proc SPIE 9909
Males, J.R., Close, L.M., et al. (2018), Proc SPIE 10703
Milli, J. et al. (2018) Proc 10703
Miller, K., et al. (2018) proc SPIE 10703
Morzinski, K. et al. (2015) ApJ 815, 108
Morzinski, K. et al. (2016) Proc SPIE 9909;
N'Diaye, M. et al. (2017) Proc AO4ELT 5
N'Diaye, M. et al. (2018) Proc SPIE 10703
Obereder, A. et al. (2018) Proc SPIE 10703
Oberti, S. et al (2018) Proc SPIE 10703
Otten, G. et al. (2017) ApJ 834, 175
Park, Ryeojin; Close, Laird M.; Siegler, Nick; Nielsen, Eric L.; Stalcup, Thomas, 2006 PASP 118 159
Rigaut, Francois; Neichel, Benoit; Bec, Matthieu; Boccas, Maxime; Garcia-Rissmann, Aurea; Gratadour, Damien, 2010 1st AO4ELT conference - Adaptative Optics for Extremely Large Telescopes, held 22-26 June, 2009 in Paris, France. Edited by Y. Clénet, J.-M. Conan, Th. Fusco, and G. Rousset. EDP Sciences id.08001
Racine, R. et al. "Speckle Noise and the Detection of Faint Companions". PASP, 111, 587 (1999).

Riccardi et al. “The adaptive secondary mirror for the Large Binocular Telescope: results of acceptance laboratory test,” 2008 Proc SPIE 7015, 701512
Riccardi et al. “The adaptive secondary mirror for the Large Binocular Telescope: optical acceptance test and preliminary on-sky commissioning results,” 2010 Proc SPIE 7736, 77362C
Riguat, F. (2015) PASP Publications of the Astronomical Society of Pacific, Volume 127, Issue 958, pp. 1197-1203
Roddier, F. 1999, Adaptive Optics in Astronomy, Cambridge Press.
Rodigas, T.J. et al. (2015) ApJ 798, 96
Rodigas, T.J. et al. (2016) ApJ 818, 106
Roggemann M.C. & J. A. Meinhardt. “Image Reconstruction By Means of Wave-Front Sensor Measurements in Close-Loop Adaptive-Optics Systems.” JOSA, Vol 10, No. 9, 1996 (1993).
Sallum, S.; Follette, K. B.; Eisner, J. A.; Close, L. M.; Hinz, P.; Kratter, K.; Males, J.; Skemer, A.; Macintosh, B.; Tuthill, P.; Bailey, V.; Defrère, D.; Morzinski, K.; Rodigas, T.; Spalding, E.; Vaz, A.; Weinberger, A. J. NATURE, 527, 342
Salama, M. et al. 2016; Proc SPIE 9909;
Salinas, R. , A. Alabi, T. Richtler, R. R. Lane 2015 A&A 577, 59
Schaller, E. L., Brown, M. E., Roe, H. G., Bouchez, A. H., Trujillo, C. A. 2006, Icarus, 184, 517S.
Schatz L. et al. (2018) proc SPIE 10703
Veran, J.P. et al. “Estimation of the Adaptive Optics Long-Exposure Point-Spread Function Using Control Loop Data.” JOSA, Vol 14, No. 11, 3057 (1997).
Thalmann, C., et al. (2015) ApJ 808, 41
Wagner, K. et al. (2018), ApJ Lett, in prep.
Wu Y-L., Close, L.M. et al. 2013 ApJ 774, 45
Wu Y-L,. Close, L.M. et al. 2015a ApJ 801, 4
Wu Y-L,. Close L.M., et al. 2015b ApJ Lett 807, 13L
Wu Y-L,. Close L.M. et al. 2016 ApJ 823, 24
Wu, Ya-Lin; Sheehan, Patrick D.; Males, Jared R.; Close, Laird M.; Morzinski, Katie M.; Teske, Johanna K.; Haug-Baltzell, Asher; Merchant, Nirav; Lyons, Eric; (2017a) ApJ 836, 223
Wu, Ya-Lin; Smith, Nathan; Close, Laird M.; Males, Jared R.; Morzinski, Katie M. (2017b) ApJ Lett 841, L7
Wu, Ya-Lin; Close, Laird M.; Kim, Jinyoung Serena; Males, Jared R.; Morzinski, Katie M. (2017c) ApJ 854, 144
Van Gorkom K., et al. (2018) proc SPIE 10703